Current Biology, Volume *28*

Supplemental Information

The Iceman's Last Meal Consisted of Fat, Wild Meat, and Cereals

Frank Maixner, Dmitrij Turaev, Amaury Cazenave-Gassiot, Marek Janko, Ben Krause-Kyora, Michael R. Hoopmann, Ulrike Kusebauch, Mark Sartain, Gea Guerriero, Niall O'Sullivan, Matthew Teasdale, Giovanna Cipollini, Alice Paladin, Valeria Mattiangeli, Marco Samadelli, Umberto Tecchiati, Andreas Putzer, Mine Palazoglu, John Meissen, Sandra Lösch, Philipp Rausch, John F. Baines, Bum Jin Kim, Hyun-Joo An, Paul Gostner, Eduard Egarter-Vigl, Peter Malfertheiner, Andreas Keller, Robert W. Stark, Markus Wenk, David Bishop, Daniel G. Bradley, Oliver Fiehn, Lars Engstrand, Robert L. Moritz, Philip Doble, Andre Franke, Almut Nebel, Klaus Oeggl, Thomas Rattei, Rudolf Grimm, and Albert Zink


A
1 mm
B

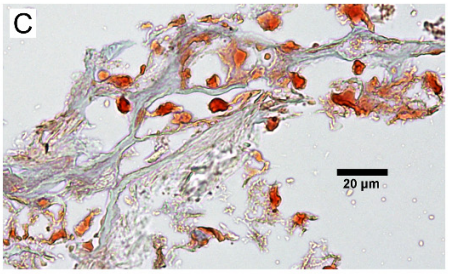
C
20 µm


D
G
E
H
F
I

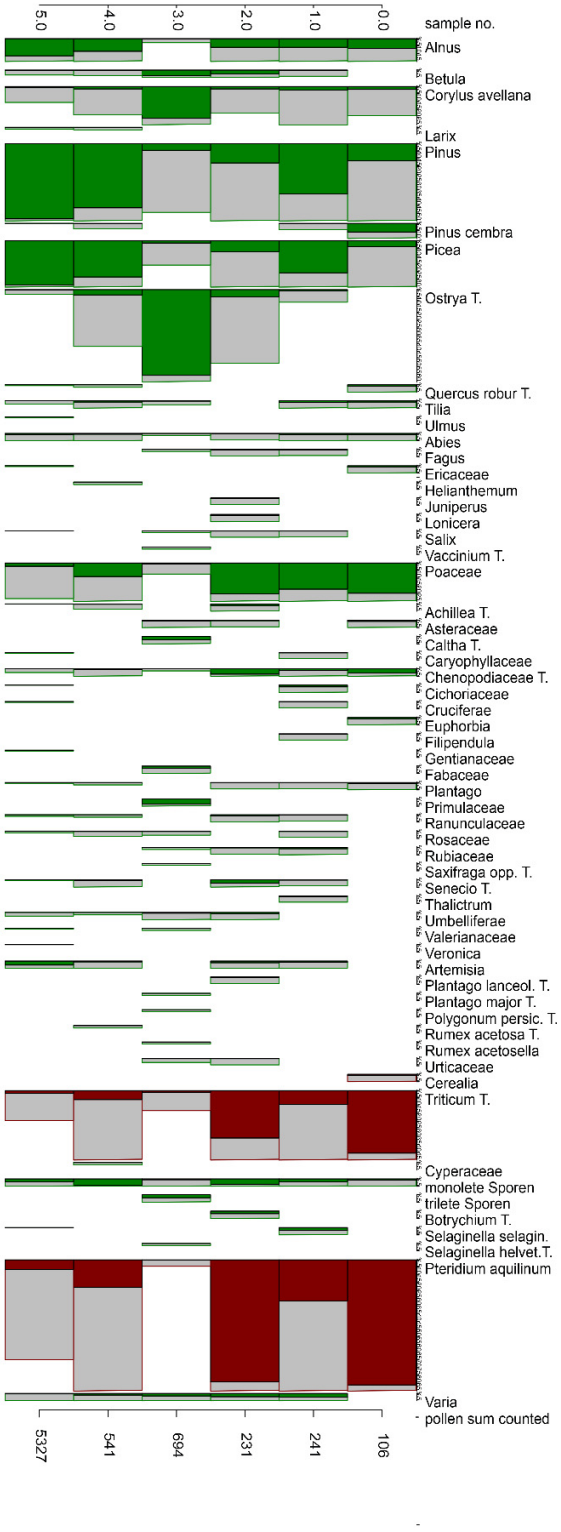
J
5.0
4.0
3.0
2.0
1.0
0.0
sample no.
Alnus
Betula
Corylus avellana
Larix
Pinus
Pinus cembra
Picea
Ostrya T.
Quercus robur T.
Tilia
Ulmus
Abies
Fagus
Ericaceae
Helianthemum
Juniperus
Lonicera
Salix
Vaccinium T.
Poaceae
Achillea T.
Asteraceae
Caltha T.
Caryophyllaceae
Chenopodiaceae T.
Cichoriaceae
Cruciferae
Euphorbia
Filipendula
Gentianaceae
Fabaceae
Plantago
Primulaceae
Ranunculaceae
Rosaceae
Rubiaceae
Saxifraga opp. T.
Senecio T.
Thalictrum
Umbelliferae
Valerianaceae
Veronica
Artemisia
Plantago lanceol. T.
Plantago major T.
Polygonum persic. T.
Rumex acetosa T.
Rumex acetosella
Urticaceae
Cerealia
Triticum T.
Cyperaceae
monolete Sporen
trilete Sporen
Botrychium T.
Selaginella selagin.
Selaginella helvet.T.
Pteridium aquilinum
Varia
pollen sum counted
5327
541
694
231
241
106

Figure S1: Animal and plant remains detected in the Iceman stomach content. Related to Figure 1. (A) Two large bundles of muscle fibers. Confocal laser scanning microscopy image. The scale bar indicates 1mm. **(B)** Magnified image of one muscle fibre bundle of Figure S1 A. The scale bar indicates 20µm. The long cylindrical unbranched muscle cells often appear in bundles and still display striated fiber structures running perpendicular to the long fiber axis characteristic for cardiac and skeletal muscle tissue. **(C)** Sudan III-stained adipose tissue. The animal remains in the cryosections display all characteristics of adipose tissue, loose connective tissue composed of Sudan III stained adipocytes. The scale bar indicates 20µm. **(D)** Apex of a wheat (*Triticum*) grain. The scale bar indicates 500µM. **(E)** Wheat (*Triticum*) bran. The scale bar indicates 100µM. **(F)** Fragment of a wheat (*Triticum*) glume. The scale bar indicates 100µM. **(G)** Sporangia of bracken (*Pteridium aquilinum*), scale bar indicates 100µM. **(H)** Spruce needle (*Picea*), one black scale bar corresponds to 5 mm. **(I)** Unidentified tissue. The scale bar indicates 100µM. The majority of plant macro remains in the Iceman`s stomach content belongs to cereal bran. Most prominent tissue types are pericarp and seed coat (testa) fragments, some glume and spikelet parts of wheat (*Triticum*). The pericarp and testa tissues belong to the *Triticum/Secale* type, characterized by a tube cell layer in the fruit wall. Given that rye (*Secale*) was not cultivated in Central Europe during the Copper Age and the pericarp fragments show the tube cell pattern all over, the bran derives from einkorn (*Triticum monococcum*), a diploid wheat. Archaeology also confirms the general presence of einkorn in the Eastern Italian Alps during the Iceman´s time [S1]. The occurrence of bracken (*Pteridum aquilinum*) sporangia is very surprising, as is a spruce (*Picea*) needle (leaf). Bracken was so far only detected in the Iceman´s intestinal contents and not reported in another Iceman archeological context. **(J)** Percentage diagram of the pollen content in the ingesta of the gastro-intestinal tract of the Iceman. All arboreal and non-arboral pollen constitute 100%. Spores are excluded from the 100%, calculated and plotted in percentages with regard to this 100% sum. Pollen in brown colour display intentional, in green unintentional consumed pollen. In total six samples from different consecutive locations of the intestinal tract are at disposal for insights in the Iceman`s nutrition habits. They were extracted: one each from the gaster (sample no. 0.0) and the lower small bowel (sample no. 1.0), as well as two each from the upper large (sample no. 2.0 and 3.0) and lower large intestine (sample no. 4.0 and 5.0). The three pollen spectra from the gaster, small bowel and the upper large bowel (sample nos 0.0 – 2.0) are dominated by bracken (*Pteridum aquilinum*) spores and pollen grains from wheat (*Triticum*-type) (brown curves, sample nos 0.0 – 2.0). Both taxa are consistently represented in the subsequent three samples of the upper and lower large bowel (sample nos 3.0 – 5.0). Their occurrence in high percentage values suggests intentional ingestion of parts of these plants [S2-S4]. The residual pollen (highlighted in green) is unintentionally ingested by respiration or drinking water and reflects the ambient vegetation the Iceman moved around. Most of these pollen types are in high quantities airborne and reflect the inneralpine forests (*Pinus, P. cembra, Picea, Larix Ostrya*-type) and grasslands (*Poaceae*) of the Ötztal Mountains. Besides these arboreal pollen types, there are also several herbal pollen types recorded. The airborne pollen of the goosefoot family (*Chenopodiaceae*-type) occurs in constant percentage values (up to 5%), similarly to mugwort (*Artemisa*) and plantain (*Plantago*, *P.*

lanceolata-type, *P. major*-type). They represent common weeds of rural sites and might have been consumed unintentionally with cereals. About 15 of the observed herbal pollen types are insect-pollinated and occur regularly in low quantities (<2%) like in the natural pollen rain. Only two types are reflected in higher percentage values in the pollen diagram: *Caltha*-type and *Primulaceae*. The first one comprises also pollen from Marsh Marigold (*Caltha palustris*) and the second type includes Cowslip, Oxlip and Primrose (*Primula veris, elatior, vulgaris*), which are edible and used as drugs in herbal medicine. However, the mentioned species of both pollen types thrive on waterlogged sites and along rivulets, which makes unintentional ingestion by drinking water plausible [S3].

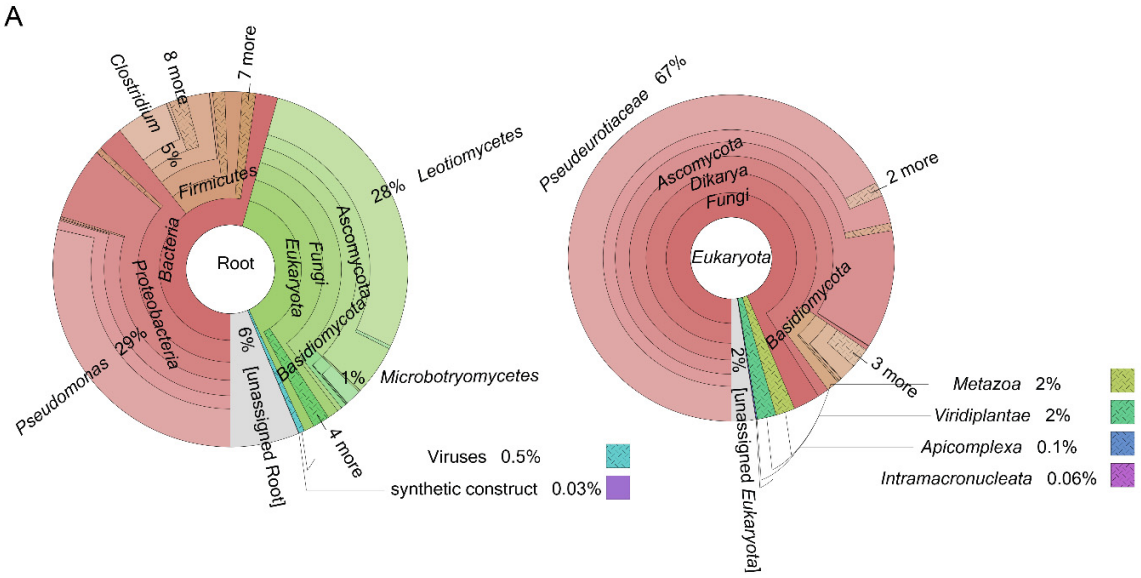

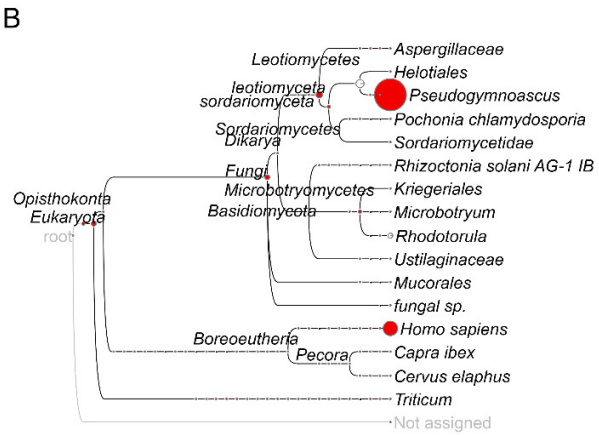

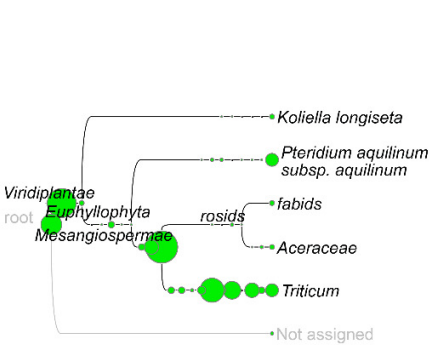

D

		Caprinae	Capra	Capra ibex	Capra hircus	Cervinae	Cervus	Cervus elaphus	Dennstaedtiaceae	Pteridium aquilinum	Triticeae	Triticum	Malvids	Aceraceae	Fabids	Ericaceae
Stomach	D0144*	11.0	7.5	0.9	0.0	1.9	0.5	0.0	2.4	2.4	0.5	0.2	0.0	0.0	0.0	0.0
	A1141	21.1	0.0	0.0	0.0	0.0	0.0	0.0	0.0	0.0	0.0	0.0	0.0	0.0	0.0	0.0
	B0624	214.6	151.8	8.6	0.0	19.1	5.3	3.9	1.1	1.1	2.5	0.9	0.3	0.0	0.0	0.0
	D0774*	210.3	139.8	10.1	0.7	21.0	5.0	4.1	0.8	0.8	3.2	1.2	0.0	0.0	0.0	0.0
	B0626	75.8	54.4	4.9	0.0	17.5	5.2	4.3	3.5	3.3	7.1	2.7	0.4	0.4	0.5	0.0
	D0775*	77.9	52.5	4.2	0.0	18.8	5.0	4.1	2.5	2.4	6.5	2.7	0.0	0.0	0.0	0.0
	A1142	37.8	30.3	0.0	0.0	0.0	0.0	0.0	0.0	0.0	0.0	0.0	0.0	0.0	0.0	0.0
	A1145	10.6	6.8	0.8	0.0	0.0	0.0	0.0	0.4	0.4	0.4	0.0	0.0	0.0	0.0	0.4
	D0145*	31.6	21.0	1.6	0.0	2.5	0.0	0.0	0.3	0.3	0.9	0.3	0.0	0.0	0.0	0.0
	A1146	13.8	9.5	1.9	0.0	4.6	1.1	0.8	0.0	0.0	0.0	0.0	0.3	0.0	0.0	0.0
	B0623	27.9	20.0	1.1	0.0	2.3	0.0	0.0	0.3	0.3	0.6	0.2	0.0	0.0	0.1	0.0
	A1144	69.6	41.1	4.5	0.0	9.0	3.0	0.0	1.0	1.0	4.0	2.5	0.0	0.0	0.0	0.0
	B0620	189.7	134.7	6.9	0.0	16.3	3.9	2.8	0.2	0.2	1.9	0.6	0.0	0.0	0.2	0.0
	D0776*	167.5	111.5	8.4	0.7	14.3	3.9	3.0	0.0	0.0	2.7	1.1	0.0	0.0	0.0	0.0
	D0777*	127.4	85.9	7.0	0.5	18.7	5.2	4.3	4.1	3.8	2.5	0.9	0.0	0.0	0.0	0.0
	A1140	8.9	5.9	0.7	0.0	0.3	0.0	0.0	0.3	0.1	0.1	0.1	0.0	0.0	0.0	0.0
	B0622	18.4	12.6	0.0	0.0	3.2	0.0	0.0	0.5	0.4	1.3	0.6	0.2	0.0	0.0	0.0
Small intestine	B0621	16.9	11.7	0.6	0.0	1.7	2.8	0.0	2.8	2.4	1.3	0.3	0.0	0.0	0.2	0.0
Upper large itestine	C1824	0.8	0.0	0.0	0.0	0.0	0.0	0.0	2.1	1.9	0.3	0.0	0.0	0.0	0.0	0.0
	C1825*	0.8	0.6	0.0	0.0	0.0	0.0	0.0	2.1	2.0	0.0	0.0	0.0	0.0	0.0	0.0
Lower large itestine	B0625	23.7	15.4	1.2	0.0	4.2	1.0	0.8	24.1	22.9	5.6	0.0	7.6	5.0	0.0	0.0
Muscle tissue	C0004	0.0	0.0	0.0	0.0	0.0	0.0	0.0	0.0	0.0	0.0	0.0	0.0	0.0	0.0	0.0
	C0005*	0.0	0.0	0.0	0.0	0.0	0.0	0.0	0.0	0.0	0.0	0.0	0.0	0.0	0.0	0.0
Extraction blank	B0629	0.0	0.0	0.0	0.0	0.0	0.0	0.0	0.0	0.0	0.0	0.0	0.0	0.0	0.0	0.0

Figure S2: Metagenomic analysis of the Iceman`s gastrointestinal tract content shotgun datasets. Related to Figure 2. (A)** Taxonomic overview of the sequence reads in a selected Illumina dataset (B0626) of the Iceman`s stomach content. Both the full taxonomic overview over all Kingdoms (left) and an overview over the Eukaryotic taxa (right) are displayed. The metagenomic reads were taxonomically assigned using the RAPSearch2 tool [S5] against the NCBI non-redundant protein database. We subjected in addition to the Iceman stomach content (B0626) the Illumina datasets of the small intestine content (B0621), the upper large intestine content (C1824), the lower large intestine content (B0625) and of the Iceman muscle tissue (C0004) to this first taxonomic profiling (the Krona plots of the latter four samples are not shown). The majority of sequence reads (between 54% and 97% of all reads) in both the Iceman's gastrointestinal tract content samples and in the Iceman muscle tissue sample were taxonomically assigned to *Bacteria* (Figure 2A). In all datasets the bacterial fraction of reads is highly dominated by the phyla *Firmicutes* (up to 83% of the *Bacteria* reads) and *Proteobacteria* (up to 94% of the *Bacteria* reads) with the genera *Clostridium* (up to 70% of the *Firmicutes* reads) and *Pseudomonas* (up to 77% of the *Proteobacteria* reads) being the major representatives of these phyla. The presence of *Clostridium* and *Pseudomonas* in Iceman`s intestinal and tissue samples has been reported already in previous molecular studies including the Iceman genomic survey [S6-S9]. The presence of the DNA of these two major genera in both the Iceman`s gastrointestinal contents and the muscle and bone tissues suggests that the *Clostridia* and *Pseudomonas* bacteria display remnants of the post-mortem colonizing bacterial community, which was shortly after the Iceman`s death involved in the overall body decomposition before the degradation has been stopped by the natural mummification and desiccations processes [S10-S13]. Beside this high fraction of bacterial reads, only 39% or less of reads in the Iceman samples were eukaryotic of which the majority (between 94% and 42%) were identified as fungal. The *Metazoa* and *Virdiplantae* reads, important for the dietary reconstruction, comprised only 0.7% to 0.2% of all reads. The Metazoan fraction of reads is highly dominated by *Primates* sequences (between 55% and 78% of *Metazoa* reads) and reads that were assigned to the *Ruminantes* (between 4% and 17% of *Metazoa* reads). We could demonstrate in one of our previous studies that the *Primates* sequences in the stomach content are human reads that match the Iceman haplotype [S14]. Most presumably, all biomolecules including the Iceman`s DNA were released post-mortem from the epithelial cells into the intestinal contents. The highest faction of plant DNA included reads that belong to the *Poaceae* family (between 26% and 85% of the *Viridiplantae* reads). Importantly, the *Ruminantes* and *Poaceae* reads possibly comprising the Iceman's animal and plant diet were only detected in the intestinal contents and not in the control muscle sample. **(B&C) Taxonomic overview of the mitochondrial **(B)** and chloroplast **(C)** sequence reads in one selected Illumina dataset (B0626) of the Iceman`s stomach content. The metagenomic reads were first assembled against the currently available complete mitochondrial and chloroplast genomes from the NCBI-nt database using BWA [S15]. Subsequently we performed a sequence similarity search of all mapped reads using blastn [S16] and the complete NCBI-nt database [S17]. Blast results were taxonomically assigned using MEGAN6 [S18]. **(D)** Animal subfamilies/genera/species and plant

families/genera/species detected in all shotgun datasets by comparison of the shotgun reads against the complete mitochondrial and chloroplast genomes in the NCBI database. The color gradient displays the number of unambiguously assigned animal and plant reads per million metagenomics reads. Control metagenomic datasets of the Iceman's muscle tissue and of the extraction blank were included in the analysis. In agreement with our previous observation the majority of reads in both the shotgun datasets of the intestine contents and of the muscle control sample were assigned to the mitochondrial genomes of various fungal species and of the Iceman (C). However, when we focus on the reads assigned to the non–human mammalian reads we detect mitochondrial reads unambiguously assigned to the animal subfamilies *Caprinae* and *Cervinae* only in the Iceman`s intestinal contents and not in the control samples (Iceman`s muscle tissue and Extraction blank) (Figure S2B and S2D). Furthermore, unambiguously assigned species-specific reads indicate the presence of both mitochondrial genomic DNA of the ibex (*Capra ibex*) and of the red deer (*Cervus elaphus*). There exists archaeological evidence that both domesticated and wild animals including red deer were part of the general Copper Age diet in the Iceman´s territories [S19]. Ibex bones, however, were not yet found in nearby Copper Age settlements. The slaughtering of high altitude animals such as the ibex directly at the hunting place may explain this confounding result. In comparison to the high fungal and human background indicated with e.g. the mitochondrial genomic reads, the plant-derived contamination seems to be relatively low. Based on our taxonomic assignment of the chloroplast reads, we detected, in all intestinal contents and the muscle tissue dataset, reads of the green algae *Koliella longiseta* (Figure S2C and S2D). Species of the genus *Koliella* grow in freshwater, but some thrive also in layers of alpine glaciers and snow [S20]. Therefore, we hypothesize that the green algae entered post-mortem the Iceman`s tissue and intestinal contents from the surrounding ice and snow. Beside this environmental algal background there are several other chloroplast reads detected solely in the Iceman`s intestine content samples (Figure S2C and S2D). Almost all intestinal content datasets contain chloroplast reads unambiguously assigned to the plant families *Dennstaedtiaceae* and *Triticeae*. Furthermore, our taxonomic assignment indicates that most *Dennstaedtiaceae* and *Triticeae* reads belong to the species *Pteridium aquilinum subsp. aquilinum* and to members of the genus *Triticum*, respectively. Few selected intestinal content datasets contain in addition chloroplast reads assigned to the *Malvids*, *Aceraceae*, *Fabids* and *Ericaceae*. However, it was not possible to taxonomically assign the latter reads further down to the genus- or species-level.

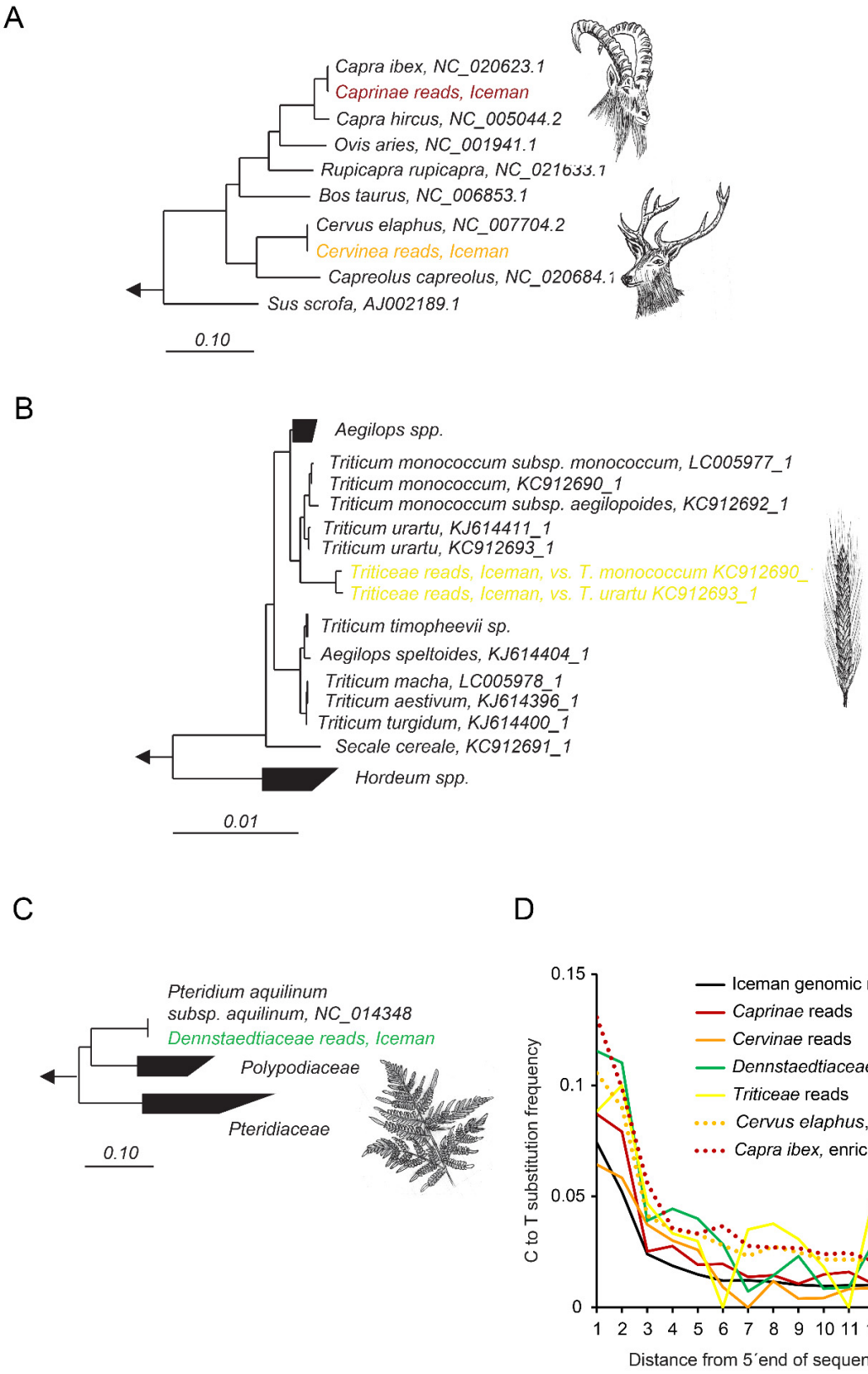
A
Capra ibex, NC_020623.1
Caprinae reads, Iceman
Capra hircus, NC_005044.2
Ovis aries, NC_001941.1
Rupicapra rupicapra, NC_021633.1
Bos taurus, NC_006853.1
Cervus elaphus, NC_007704.2
Cervinea reads, Iceman
Capreolus capreolus, NC_020684.1
Sus scrofa, AJ002189.1
0.10
B
Aegilops spp.
Triticum monococcum subsp. monococcum, LC005977_1
Triticum monococcum, KC912690_1
Triticum monococcum subsp. aegilopoides, KC912692_1
Triticum urartu, KJ614411_1
Triticum urartu, KC912693_1
Triticeae reads, Iceman, vs. T. monococcum KC912690_1
Triticeae reads, Iceman, vs. T. urartu KC912693_1
Triticum timopheevii sp.
Aegilops speltoides, KJ614404_1
Triticum macha, LC005978_1
Triticum aestivum, KJ614396_1
Triticum turgidum, KJ614400_1
Secale cereale, KC912691_1
Hordeum spp.
0.01
C
Pteridium aquilinum
subsp. aquilinum, NC_014348
Dennstaedtiaceae reads, Iceman
Polypodiaceae
Pteridiaceae
0.10
D
0.15
0.1
0.05
0
C to T substitution frequency
1 2 3 4 5 6 7 8 9 10 11 12 13 14 15
Distance from 5´end of sequence read
Iceman genomic reads
Caprinae reads
Cervinae reads
Dennstaedtiaceae reads
Triticeae reads
Cervus elaphus, enriched
Capra ibex, enriched

Figure S3: Phylogenetic assignment of the reconstructed plastid genomes and DNA damage pattern analysis of the unambiguously assigned plastid reads. Related to Figure 2 and Data S1. (A) Phylogenetic assignment of the two complete animal mitochondrial genomes reconstructed from the *Caprinae* and *Cervinae* reads. A total of 16208 informative nucleotide positions were used for the phylogenetic analysis. The comparative dataset included complete mitochondrial genomes of selected wild and domesticated ungulates (NCBI Accession Numbers are provided in the figure). The arrow indicates the outgroup (*Equus caballus* NC_001640.1, *Equus asinus* NC_001788.1). The two complete animal mitochondrial genomes reconstructed from the Caprinae and Cervinae reads were phylogenetically assigned to the ibex (*Capra ibex*) and red deer (*Cervus elaphus*) mitogenomes. **(B)** Phylogenetic assignment of the two partial plant mitochondrial genomes reconstructed from the *Triticeae* reads. A total of 17357 informative nucleotide positions were used for the phylogenetic analysis. The comparative dataset included complete chloroplast genomes of selected members of the *Triticeae* tribe (NCBI Accession Numbers are provided in the figure). The outgroup (*Phleum alpinum* KM974747.1, *Poa palustris* KM974749.1) is indicated by the arrow. Both chloroplast genomes partially reconstructed from the *Triticeae* reads clustered together and were closely assigned to chloroplast genomes of *Triticum monococcum* and *Triticum urartu.* However, the presence of two different *Triticum* chloroplast genomes, as indicated by the FastQ Screen analysis (see Data S1_ FastQScreen Triticeae reads), is not supported by the phylogenetic analysis. Visual inspection of the *Triticum* chloroplast alignment revealed that the *T. urartu* and *T. monococcum* species specific reads that were identified by FastQ Screen were all aligned to sequence motifs that are unique to two modern reference sequences (KC912690, KC912693) published together in a previous study [S21]. These specific sequence motifs are not shared with any other currently available *T. urartu* and *T. monococcum* chloroplast genome. Therefore, we decided not to consider these unique insertions in the phylogenetic assignment. **(C)** Phylogenetic assignment of the partial plant mitochondrial genomes reconstructed from the *Dennstaedtiaceae* reads**.** A total of 56972 informative nucleotide positions were used for the phylogenetic analysis. The comparative dataset included complete chloroplast genomes of selected members of the *Dennstaedtiaceae, Polypodiaceae,* and *Pteridiaceae* (NCBI Accession Numbers are provided in the figure). The outgroup (*Alsophila spinolosa* FJ556581.1, *Plagiogyria glauca* KP136831.1, *Marsilea crenata* KC536646.1) is indicated by the arrow. The partial plant mitochondrial genomes reconstructed from the *Dennstaedtiaceae* reads were phylogenetically assigned to the *Pteridium aquilinum subsp. aquilinum* chloroplast genome. **(D)** Comparison of the cytosine to thymine substitution frequency in the 5´end of the validated animal mitochondrial, plant chloroplast and Iceman human sequence reads detected in the Iceman stomach content. The cytosine deamination pattern of the *Caprinae* and *Cervidae* reads extracted from the metagenomic dataset are highlighted in red and orange, respectively. Damage patterns of the enriched animal plastid reads are displayed with dotted lines. Damage patterns of the *Triticeae* and *Dennstaedticaeae* reads are depicted in yellow and green lines, respectively. The cytosine deamination pattern of the human reads detected in the Iceman stomach content metagenome is highlighted as a black line. All mitochondrial and chloroplast reads (non-UDG treated) extracted

from the four dominant animal and plant (sub)families *Caprinae Cervinae, Dennstaedtiaceae*, and *Triticeae* and the enriched animal plastid reads display an increased C to T misincorporation pattern at the 5′ end indicative of ancient DNA. The detected 5′ C to T substitution frequencies are in the same range (~12% to 6%) as the 5′cytosine deamination pattern (~7%) of the human reads detected in the Iceman stomach content. The C to T misincorporation pattern in the animal and plant reads was not restricted to the 5′ end and was found additionally within the reads. We hypothesize that this effect comes most probably from the much lower number of available animal and plant reads compared to the highly abundant Iceman genomic reads.

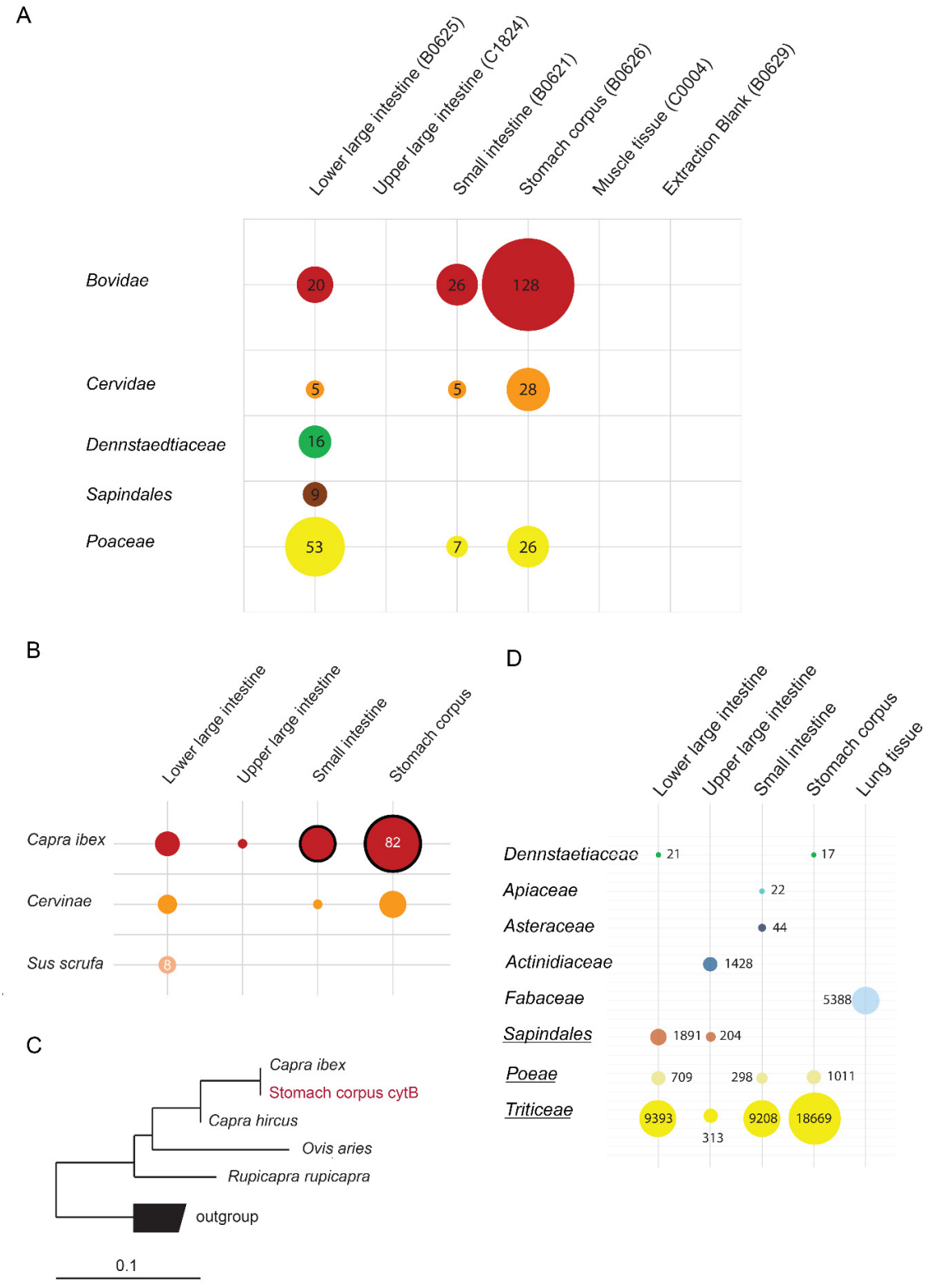
A
Lower large intestine (B0625)
Upper large intestine (C1824)
Small intestine (B0621)
Stomach corpus (B0626)
Muscle tissue (C0004)
Extraction Blank (B0629)
Bovidae
Cervidae
Dennstaedtiaceae
Sapindales
Poaceae
20
26
128
5
5
28
16
9
53
7
26
B
Lower large intestine
Upper large intestine
Small intestine
Stomach corpus
Capra ibex
Cervinae
Sus scrufa
82
8
C
Capra ibex
Stomach corpus cytB
Capra hircus
Ovis aries
Rupicapra rupicapra
outgroup
0.1
D
Lower large intestine
Upper large intestine
Small intestine
Stomach corpus
Lung tissue
Dennstaetiaceae
Apiaceae
Asteraceae
Actinidiaceae
Fabaceae
Sapindales
Poeae
Triticeae
21
17
22
44
1428
5388
1891
204
709
298
1011
9393
313
9208
18669

Figure S4: DNA-barcode analysis of the Iceman gastrointestinal content samples and control samples. Related to Figure 2. (A) Animal families and plant families/orders detected in the Iceman intestinal contents by comparison of selected shotgun read datasets against the DNA barcodes deposited in the BOLD system database (http://www.boldsystems.org/). The DNA barcodes deposited at the BOLD database [S22] comprise fragments of the cytochrome c oxidase I (COI) gene, the ribulose bisphosphate carboxylase (*rbcL*) gene and the maturase K (*matK*) gene. The comparative analysis were performed against the COI fragments deposited in the groups *Mammalia, Actinopterygii*, *Astacidae, Nematoda*, and *Platyhelmintes* and against the *rbcL* and *matK* fragments in the groups *Magnoliophyta*, *Pinophyta*, *Bryophyta*, *Pteridophyta*. The bubble sizes correspond to the number of unambiguously assigned reads. Importantly, this further taxonomic assignment of the reads against the DNA barcodes provides no evidence for further yet missed components of the Iceman`s diet. All previously detected major animal and plant groups present in the Iceman`s last meals were confirmed at the family and order level. **(B)** Animal species and sub-family detected in the Iceman intestinal contents with the 12S rRNA amplicon assignment to the NCBI nt database. Bubble size corresponds to the number of unambiguously assigned reads. Results confirmed by the *cytB* amplicons are framed with a black circle. **(C)** Phylogenetic assignment of the Iceman *cytB* amplicon sequence to *cytB* sequences of domesticated and wild representatives of the family *Caprinae* known to be present in the European Alpine area during the Iceman's time [S19]. The tree calculations were performed using the maximum-likelyhood algorithm (PhyML) implemented in the ARB software package [S23]. A total of 198 informative DNA positions were used for the analysis. Two cytB sequences from the genus *Bos* spp, were used as outgroup. The *cytB* sequence detected in the Iceman stomach corpus content is highlighted in red. The bar indicates 10% estimated sequence divergence. The majority of the 12S rRNA amplicons (99.2-99.7%) were assigned to the human 12S rRNA gene variant. This result came not unexpected considering the high amount of Iceman human genome reads already detected in our previous study in the stomach content [S14]. We hypothesize that the Iceman genetic material penetrated post-mortem after cell lysis into the stomach content. Most other non-human mammalian 12S rRNA amplicons were in all analyzed intestinal content unambiguously assigned to the ibex (*Capra ibex*) and the deer family (*Cervinae*), thereby supporting the results of the metagenomic analysis. The presence of ibex DNA was further confirmed by the analysis of the cytB amplicons. We detected in both contents of the stomach and the small intestine the amplified fragments of the cytB gene that were phylogenetically assigned to the cytB gene fragment of the ibex (*Capra ibex*). Interestingly, the 12S rRNA amplicon data indicates the presence of DNA of the domesticated pig (*Sus scrofa*). However, since this result was not supported by any other analysis pipeline (metagenomics, proteomics), we decided not to consider it as part of the Iceman`s diet. **(D)** Plant order, tribes and families detected in the Iceman intestinal contents with the *trnL* amplicon assignment to the NCBI nt database. Bubble size corresponds to the number of unambiguously assigned reads. The order, tribes and families confirmed by the *rbcL* amplicons are highlighted with underlined names. The analysis of the *trnL* and *rbcl* amplicons confirms our previous metagenomics results on the presence of plant DNA assigned to the families

Denstaedticaceae and *Triticeae*. However, beside these two families numerous other plant tribes and families were detected in the Iceman intestinal contents with the *trnL* and rbcL amplicon assignment to the NCBI nt database. The absence of the detected plant order, tribes and families in the Iceman`s lung tissue control sample argues against an external contamination of the intestine contents during sampling or DNA extraction via pollen or plant DNA. However, the relative contribution of pollen and macrofossils to the total DNA yield and latter obtained molecular results in these and other ancient specimen remains to be determined [S24].

Supplemental References

S1. Festi, D., Tecchiati, U., Steiner, H., and Oeggl, K. (2011). The Late Neolithic settlement of Latsch, Vinschgau, northern Italy: subsistence of a settlement contemporary with the Alpine Iceman, and located in his valley of origin. Vegetation history and archaeobotany *20*, 367.

S2. Dickson, J.H., Oeggl, K., Holden, T.G., Handley, L.L., O'Connell, T.C., and Preston, T. (2000). The omnivorous Tyrolean Iceman: colon contents (meat, cereals, pollen, moss and whipworm) and stable isotope analyses. Philos Trans R Soc Lond B Biol Sci *355*, 1843-1849.

S3. Oeggl, K. (2000). The Diet of the Iceman. In. Bortenschlager S., Oeggl K., editors The Iceman and his natural environment. The Man in the Ice. *4*, 89-115.

S4. Oeggl, K., Kofler, W., Schmidl, A., Dickson, J.H., Egarter-Vigl, E., and Gaber, O. (2007). The reconstruction of the last itinerary of "Ötzi", the Neolithic Iceman, by pollen analyses from sequentially sampled gut extracts. Quaternary Science Reviews *26*, 853 - 861.

S5. Zhao, Y., Tang, H., and Ye, Y. (2012). RAPSearch2: a fast and memory-efficient protein similarity search tool for next-generation sequencing data. Bioinformatics *28*, 125-126.

S6. Cano, R.J., Tiefenbrunner, F., Ubaldi, M., Del Cueto, C., Luciani, S., Cox, T., Orkand, P., Kunzel, K.H., and Rollo, F. (2000). Sequence analysis of bacterial DNA in the colon and stomach of the Tyrolean Iceman. Am J Phys Anthropol *112*, 297-309.

S7. Keller, A., Graefen, A., Ball, M., Matzas, M., Boisguerin, V., Maixner, F., Leidinger, P., Backes, C., Khairat, R., Forster, M., et al. (2012). New insights into the Tyrolean Iceman's origin and phenotype as inferred by whole-genome sequencing. Nat Commun *3*, 698.

S8. Maixner, F., Thomma, A., Cipollini, G., Widder, S., Rattei, T., and Zink, A. (2014). Metagenomic analysis reveals presence of Treponema denticola in a tissue biopsy of the Iceman. PLoS One *9*.

S9. Rollo, F., Luciani, S., Canapa, A., and Marota, I. (2000). Analysis of bacterial DNA in skin and muscle of the Tyrolean iceman offers new insight into the mummification process. Am J Phys Anthropol *111*, 211-219.

S10. Daldrup, T., and Huckenbeck, W. (1984). Significance of the putrefactive bacterium Clostridium sordellii for the determination of age of the cadaver. Z Rechtsmed *92*, 121-125.
S11. Janisch, S., Gunther, D., Fieguth, A., Bange, F.C., Schmidt, A., and Debertin, A.S. (2010). Post-mortal detection of clostridia--putrefaction or infection? Arch Kriminol *225*, 99-108.
S12. Lynnerup, N. (2007). Mummies. Am J Phys Anthropol *45*, 162-190.
S13. Metcalf, J.L., Xu, Z.Z., Weiss, S., Lax, S., Van Treuren, W., Hyde, E.R., Song, S.J., Amir, A., Larsen, P., Sangwan, N., et al. (2016). Microbial community assembly and metabolic function during mammalian corpse decomposition. Science *351*, 158-162.
S14. Maixner, F., Krause-Kyora, B., Turaev, D., Herbig, A., Hoopmann, M.R., Hallows, J.L., Kusebauch, U., Vigl, E.E., Malfertheiner, P., Megraud, F., et al. (2016). The 5300-year-old Helicobacter pylori genome of the Iceman. Science *351*, 162-165.
S15. Li, H., and Durbin, R. (2010). Fast and accurate long-read alignment with Burrows-Wheeler transform. Bioinformatics *26*, 589-595.
S16. Altschul, S.F., Gish, W., Miller, W., Myers, E.W., and Lipman, D.J. (1990). Basic local alignment search tool. J Mol Biol *215*, 403-410.
S17. Coordinators, N.R. (2017). Database Resources of the National Center for Biotechnology Information. Nucleic Acids Res *45*, D12-D17.
S18. Huson, D.H., Beier, S., Flade, I., Gorska, A., El-Hadidi, M., Mitra, S., Ruscheweyh, H.J., and Tappu, R. (2016). MEGAN Community Edition - Interactive Exploration and Analysis of Large-Scale Microbiome Sequencing Data. PLoS Comput Biol *12*, e1004957.
S19. Tecchiati, U., Castiglioni, E., and Rottoli, M. (2013). Economia di sussistenza nell'età del Rame dell'Italia settentrionale. Il contributo di archeozoologia e archeobotanica. in R. C. de Marinis (a cura di), L'età del Rame: la pianura padana e le Alpi al tempo di Ötzi, Brescia: La compagnia della stampa Massetti Rodella, 87-100.
S20. Katana, A., Kwiatowski, J., Spalik, K., Zakryś, B., Szalacha, E., and Szymańska, H. (2001). PHYLOGENETIC POSITION OF KOLIELLA (CHLOROPHYTA) AS INFERRED FROM NUCLEAR AND CHLOROPLAST SMALL SUBUNIT rDNA. Journal of Phycology *37*, 443-451.
S21. Middleton, C.P., Senerchia, N., Stein, N., Akhunov, E.D., Keller, B., Wicker, T., and Kilian, B. (2014). Sequencing of chloroplast genomes from wheat, barley, rye and their relatives provides a detailed insight into the evolution of the Triticeae tribe. PLoS One *9*, e85761.
S22. Ratnasingham, S., and Hebert, P.D. (2007). bold: The Barcode of Life Data System (http://www.barcodinglife.org). Mol Ecol Notes *7*, 355-364.
S23. Ludwig, W., Strunk, O., Westram, R., Richter, L., Meier, H., Yadhukumar, Buchner, A., Lai, T., Steppi, S., Jobb, G., et al. (2004). ARB: a software environment for sequence data. Nucleic Acids Res *32*, 1363-1371.

S24. Parducci, L., Valiranta, M., Salonen, J.S., Ronkainen, T., Matetovici, I., Fontana, S.L., Eskola, T., Sarala, P., and Suyama, Y. (2015). Proxy comparison in ancient peat sediments: pollen, macrofossil and plant DNA. Philos Trans R Soc Lond B Biol Sci *370*, 20130382.

S25. Olivieri, C., Marota, I., Rizzi, E., Ermini, L., Fusco, L., Pietrelli, A., De Bellis, G., Rollo, F., and Luciani, S. (2014). Positioning the red deer (Cervus elaphus) hunted by the Tyrolean Iceman into a mitochondrial DNA phylogeny. PLoS One *9*, e100136.

S26. Fraser, R.A., Bogaard, A., Schäfer, M., Arbogast, R., and Heaton, T.H.E. (2013). Integrating botanical, faunal and human stable carbon and nitrogen isotope values to reconstruct land use and palaeodiet at LBK Vaihingen an der Enz, Baden-Württemberg. World Archaeology *45*, 492-517.

S27. Macko, S.A., Lubec, G., Teschler-Nicola, M., Andrusevich, V., and Engel, M.H. (1999). The Ice Man's diet as reflected by the stable nitrogen and carbon isotopic composition of his hair. FASEB J *13*, 559-562.

S28. Miller, N.F., Spengler, R.N., and Frachetti, M. (2016). Millet cultivation across Eurasia: Origins, spread, and the influence of seasonal climate. The Holocene *26*, 1566-1575.

S29. DeNiro, M., and Epstein, S. (1977). Mechanism of carbon isotope fractionation associated with lipid synthesis. Science *197*, 261-263.

S30. Bollongino, R., Nehlich, O., Richards, M.P., Orschiedt, J., Thomas, M.G., Sell, C., Fajkošová, Z., Powell, A., and Burger, J. (2013). 2000 Years of Parallel Societies in Stone Age Central Europe. Science *342*, 479-481.

S31. Craig, O.E., Ross, R., Andersen, S.H., Milner, N., and Bailey, G.N. (2006). Focus: sulphur isotope variation in archaeological marine fauna from northern Europe. Journal of Archaeological Science *33*, 1642-1646.

S32. Moghaddam, N., Müller, F., Hafner, A., and Lösch, S. (2016). Social stratigraphy in Late Iron Age Switzerland: stable carbon, nitrogen and sulphur isotope analysis of human remains from Münsingen. Archaeological and anthropological sciences *8*, 149-160.

S33. Nehlich, O., Fuller, B.T., Jay, M., Mora, A., Nicholson, R.A., Smith, C.I., and Richards, M.P. (2011). Application of sulphur isotope ratios to examine weaning patterns and freshwater fish consumption in Roman Oxfordshire, UK. Geochimica et Cosmochimica Acta *75*, 4963-4977.

S34. Nehlich, O., Fuller, B.T., Márquez-Grant, N., and Richards, M.P. (2012). Investigation of diachronic dietary patterns on the islands of Ibiza and Formentera, Spain: Evidence from sulfur stable isotope ratio analysis. American Journal of Physical Anthropology *149*, 115-124.

S35. Privat, K.L., O'Connell, T.C., and Hedges, R.E.M. (2007). The distinction between freshwater- and terrestrial-based diets: methodological concerns and archaeological applications of sulphur stable isotope analysis. Journal of Archaeological Science *34*, 1197-1204.

S36. Richards, M.P., Fuller, B.F., and Hedges, R.E.M. (2001). Sulphur isotopic variation in ancient bone collagen from Europe : implications for human palaeodiet, residence mobility, and modern pollutant studies. Earth and planetary science letters. *191*, 185-190.

S37. Richards, M.P., Fuller, B.T., Sponheimer, M., Robinson, T., and Ayliffe, L. (2003). Sulphur isotopes in palaeodietary studies: a review and results from a controlled feeding experiment. International Journal of Osteoarchaeology *13*, 37-45.

S38. Vika, E. (2009). Strangers in the grave? Investigating local provenance in a Greek Bronze Age mass burial using delta S-34 analysis. J Archaeol Sci 2024-2028.

S39. Hedges, R.E.M., Clement, J.G., Thomas, C.D.L., and O'Connell, T.C. (2007). Collagen turnover in the adult femoral mid-shaft: Modeled from anthropogenic radiocarbon tracer measurements. American Journal of Physical Anthropology *133*, 808-816.

S40. Cordain, L., Watkins, B.A., Florant, G.L., Kelher, M., Rogers, L., and Li, Y. (2002). Fatty acid analysis of wild ruminant tissues: evolutionary implications for reducing diet-related chronic disease. Eur J Clin Nutr *56*, 181-191.

S41. Mayer, B.X., Reiter, C., and Bereuter, T.L. (1997). Investigation of the triacylglycerol composition of iceman's mummified tissue by high-temperature gas chromatography. J Chromatogr B Biomed Sci Appl *692*, 1-6.

S42. Mirabaud, S., Rolando, C., and Regert, M. (2007). Molecular criteria for discriminating adipose fat and milk from different species by NanoESI MS and MS/MS of their triacylglycerols: application to archaeological remains. Anal Chem *79*, 6182-6192.